XLVI CILAMCE
VITÓRIA - ES - BRAZIL - 2025
XLVI IBERO-LATIN AMERICAN CONGRESS ON COMPUTATIONAL METHODS IN ENGINEERING

Validation of numerical simulation of forced convection in a ventilated cavity using OpenFOAM

Hugo K. Noel[1], Andreia A. Nascimento[1], Felipe P. Mariano[1]

[1]*Laboratório de Engenharia Térmica e de Fluidos (LATEF), Escola de Engenharia Elétrica, Mecânica e de Computação (EMC), Universidade Federal de Goiás (UFG)*
Av. Esperança, Campus Samambaia, Al. Ingá, Prédio B5, 74.690-900, Goiás/Goiânia, Brasil
hugo_kalev@discente.ufg.br, aanascimento@ufg.br, fpmariano@ufg.br

Abstract. This study presents a numerical investigation of laminar and turbulent forced convection in a square ventilated cavity. The main objective of the present work was to replicate the velocity and temperature fields from the reference studies using the OpenFOAM® software, that is free, open-source and without cost to analyze the fluid flow and heat transfer mechanisms under varying Reynolds and Prandtl numbers. The computational domain consists of a square cavity with two openings: an inlet located at the upper left side of vertical wall and an outlet at the lower right vertical wall. The flow is considered steady, incompressible, and Newtonian, with constant thermophysical properties. Boundary conditions include a uniform inlet velocity and a temperature of 299 K, while all cavity walls are assumed adiabatic. The initial temperature in the cavity is set to 300 K. Simulations were carried out using the 'buoyantSimpleFoam' solver. Numerical modifications were made to the discretization schemes and relaxation factors, differing from the original study, with the aim of assessing their impact on the stability and accuracy of the solution. The analysis includes velocity vector fields, temperature distributions, internal vortex structures, and the evaluation of local and average Nusselt numbers along the cavity walls. The results obtained are in strong agreement with those reported by references, both qualitatively and quantitatively, confirming the reliability of the implemented numerical approach. The study also reinforces the suitability of OpenFOAM® as a robust and flexible platform for simulating fluid flow with heat transfer in engineering systems, even under different numerical settings.

Keywords: Computational Fluid Dynamics, Forced convection, OpenFOAM, Ventilated cavity.

1 Introduction

The growing demand for efficient and sustainable heating, ventilation, air conditioning, and refrigeration (HVAC-R) systems has driven the development of new technologies and the optimization of existing processes. These systems play a crucial role in various industries, such as food, healthcare, and transportation—and are responsible for a significant share of the energy consumption in commercial, industrial, and residential buildings. In light of global challenges related to energy efficiency and sustainability, the optimization of HVAC-R systems has become one of the key research and development focuses in the field of thermal and fluid engineering. The increasing need for more efficient and sustainable climate control and refrigeration solutions reflects changes in energy consumption patterns and the environmental requirements imposed by global sustainability policies.

Traditional HVAC-R systems, while effective, face limitations in terms of energy efficiency, precise temperature control, and integration with renewable energy sources. Since industries that rely on HVAC-R account for a significant portion of global energy consumption, it is essential to seek alternatives that reduce environmental impact and improve system efficiency. According to Hailing Fu et al. (2024), environmental impacts and energy consumption are the main drivers for the development of new refrigeration solutions, in addition to the quality of stored products. HVAC-R systems account for 15% of global energy consumption and 70% of the energy usage within the cold chain, as reported by Niu et al. (2024). Consequently, the economic growth that fuels the expansion

of the refrigeration industry also faces challenges regarding its economic and environmental impacts. In this context, the analysis of refrigeration systems and their industrial applications has become a relevant topic, especially considering the significant impact these systems exert on energy consumption and environmental sustainability.

In the context of refrigerated space design, such as cold rooms, computational modeling has proven to be a powerful tool for performing simulations, analyzing results, and optimizing systems. It enables not only performance analysis but also the identification of improvements that can be implemented in both system design and operation. The development of new software tools—or the use of existing ones—for Computational Fluid Dynamics (CFD) simulations provides a virtual environment where multiple configurations can be tested without the need for costly physical prototypes. Moreover, the use of CFD to optimize HVAC-R systems aligns with current trends in engineering digitalization and automation. Optimization not only yields economic benefits but also results in a significant reduction in environmental impact, contributing to the achievement of global targets for reducing greenhouse gas emissions and energy consumption. The relevance of the present study, therefore, extends beyond the field of thermal engineering to encompass sustainability and energy efficiency.

In the specific context of industrial refrigeration, particularly in cold rooms, CFD techniques have proven to be essential tools for the analysis and optimization of refrigerated spaces. In the study by Castro Silva (2018), the use of FLUENT® software is highlighted for its ease of use, versatility, and efficiency in achieving solution convergence. The author emphasizes that, when comparing numerical simulations with experimental data, results obtained with FLUENT® show a smaller absolute error, indicating its accuracy in predicting the thermal performance of refrigeration equipment. Furthermore, the research underscores the inadequacy of two-dimensional simulations for these configurations, suggesting that three-dimensional simulations are more representative of the real phenomena observed.

In another study, which employed OpenFOAM software, Limane et al. (2014) investigated thermo-ventilation by analyzing airflow in a rectangular cavity with a heated floor. The validation of OpenFOAM was conducted by comparing different turbulence models and solvers with measurements previously reported in the literature. By varying parameters such as heat flux, inlet section height, and inlet airflow velocity, the authors examined their influence on the numerical solution. Overall, they concluded that the validation of OpenFOAM yielded satisfactory results when compared with the experimental data of Nielsen (1976). Additionally, Limane et al. (2017) presented a computational simulation of moist airflow, heat transfer, and mass transfer in an indoor swimming pool using OpenFOAM. This study validated the proposed numerical model by comparing it with experimental measurements of air velocity, temperature, and humidity, as well as by assessing the impact of outdoor climatic conditions and the presence of swimmers in the indoor environment. The authors concluded that OpenFOAM can be used to simulate moist airflow in large indoor environments and that swimmer activity affects the distribution of air temperature and humidity.

The objective of the present work is to investigate the application of OpenFOAM software to simulate refrigerated environments. The specific objectives include validating the use of the selected computational models and OpenFOAM for simulating the refrigeration of enclosed spaces, and identifying critical numerical parameters that influence case convergence, considering aspects such as component and environment geometry, fluid properties, and operating conditions.

2 Methodology

The validation of the adopted model and the use of OpenFOAM software for analyzing flows in cold storage chambers was carried out through comparison with the study originally conducted by Mioralli et al. (2017). This validation was performed by numerically reproducing the forced convection problem in a square ventilated cavity. Thus, to simulate forced refrigerated airflows in a confined space, the mathematical model is based on the continuity, energy balance, and Navier–Stokes equations, Eqs. (1), (2), and (3), respectively:

$$\nabla \cdot \vec{u} = 0, \tag{1}$$

$$\frac{\partial \vec{u}}{\partial t} + (\vec{u} \cdot \nabla)\vec{u} = -\frac{1}{\rho}\nabla p + \nu \nabla^2 \vec{u}, \tag{2}$$

$$\rho C_p \left(\frac{\partial T}{\partial t} + \vec{u} \cdot \nabla T\right) = k\nabla^2 T + \phi, \tag{3}$$

where $\vec{u}$ is the velocity vector; ∇ is the divergence operator; $\vec{\nabla}$ is the gradient operator; p is pressure; ν is the kinematic viscosity; ∇^2 is the Laplacian operator; $\vec{g}$ is the gravitational vector; β is the volumetric thermal expansion coefficient at the initial mean temperature; T is the fluid temperature; T_0 is the initial mean temperature; ρ is the fluid density at the initial mean temperature; C_p is the specific heat at constant pressure at the initial mean temperature; k is the thermal conductivity at the initial mean temperature; t is time; and ϕ is the viscous dissipation rate.

To compare with the work of Mioralli et al. (2017), these equations were non-dimensionalized and simplified for steady-state conditions, using the following dimensionless variables:

$$X = \frac{x}{H};\ Y = \frac{y}{H}, \tag{4}$$

$$U = \frac{u}{u_{in}}; V = \frac{v}{u_{in}}; P = \frac{p}{pu_{in}^2};\ \theta = \frac{T-T_{in}}{T-T_w}, \tag{5}$$

where H is the height of the confined space; u and v are the velocity components in the x and y directions; u_{in} is the inlet velocity; T_{in} is the inlet temperature; and Tw is the wall temperature.

Finally, the equations were simplified for two-dimensional steady-state flows, resulting in:

$$\frac{\partial U}{\partial x} + \frac{\partial V}{\partial y} = 0, \tag{6}$$

$$U\frac{\partial U}{\partial X} + V\frac{\partial U}{\partial Y} = -\frac{\partial P}{\partial X} + \frac{1}{Re}\left[\frac{\partial^2 U}{\partial X^2} + \frac{\partial^2 U}{\partial Y^2}\right], \tag{7}$$

$$U\frac{\partial V}{\partial X} + V\frac{\partial V}{\partial Y} = -\frac{\partial P}{\partial Y} + \frac{1}{Re}\left[\frac{\partial^2 V}{\partial X^2} + \frac{\partial^2 V}{\partial Y^2}\right], \tag{8}$$

$$U\frac{\partial \theta}{\partial X} + V\frac{\partial \theta}{\partial Y} = \frac{1}{Re\ Pr}\left[\frac{\partial^2 \theta}{\partial X^2} + \frac{\partial^2 \theta}{\partial Y^2}\right], \tag{9}$$

where Re is the Reynolds number and Pr is the Prandtl number.

The heat transfer rate through the cavity walls was computed via the local Nusselt number:

$$Nu_{local} = -\left.\frac{\partial \theta}{\partial n}\right|_w, \tag{10}$$

where n is the direction normal to the wall.

The Nu_{local} data were obtained using the *plotOverLine* function in ParaView, an open-source software also used for visualizing the flow fields generated in OpenFOAM. Applying first-order centered finite differences to Eq. (10) yields:

$$Nu_{local} = \frac{1}{\Delta n}\left[\frac{(T-T_{in})-(T-T_w)}{(T-T_w)}\right], \tag{11}$$

where Δn is the distance from the center of the first mesh cell to the wall, and T is the temperature at the center of each cell located Δn from the wall. Thus, a reference line is defined with *plotOverLine* Paraview command at a distance Δn from the wall, and the temperatures of the cell centers adjacent to the wall are computed.

From the local Nusselt number distribution along each wall, the mean local Nusselt number ($\overline{Nu}_{local}$) is computed for each wall. According to Mioralli et al. (2017), this average is given by:

$$\overline{Nu}_{local} = -\frac{1}{(S_{i1}-S_{i2})}\int_{S_{i1}}^{S_{i2}} Nu_i\, dS. \tag{12}$$

which can be solved numerically using the Trapezoidal Rule (Chapra and Canale, 2008). This yields:

$$\overline{Nu}_{local} = \frac{\frac{1}{2}Nu(x_0) + \sum_{i=1}^{n-1} Nu(x_i) + \frac{1}{2}Nu(x_n)}{\Delta n}, \tag{13}$$

where $Nu(x_i)$ is the Nusselt number at the center of the cell adjacent to the wall, calculated from Eq. (11), and Δn is the spacing between cell centers.

Finally, with the distribution of mean local Nusselt numbers for each wall, Mioralli et al. (2017) define the overall mean Nusselt number of the cavity as:

$$\overline{Nu} = \sum \frac{\overline{Nu}_{local}(S_{i2}-S_{i1})}{S_{total}}. \tag{14}$$

For steady-state simulations, convergence of the iterative process and pressure field satisfying mass conservation was ensured by applying under-relaxation factors for velocity, pressure, and temperature, as shown in Table 1, along with the residual values used to comparison with those of Mioralli et al. (2017).

Table 1. Under-relaxation factors and residuals applied in the simulations.

Parameter	Study	Velocity	Pressure	Temperature
Under-relaxation	Present Work	0.10	0.70	0.30
	Mioralli et al.	0.30	0.70	0.80
Residuals	Present Work	1.0×10^{-5}	1.0×10^{-5}	1.0×10^{-5}
	Mioralli et al.	1.0×10^{-4}	1.0×10^{-5}	1.0×10^{-3}

The computational domain geometry is shown in Fig. 1. The boundary conditions and physical parameters used in this study were implemented identically to those of Mioralli et al. (2017) to enable direct comparison and validation. The modeled cavity has a unit aspect ratio (H/L) and an auxiliary coordinate system "S" was defined to identify the cavity corners: wall "A" (left) corresponds to S=0–1, wall "B" (bottom) to S=1–2, wall "C" (right) to S=2–3, and wall "D" (top) to S=3–4.

The cavity has unit height, width, and depth, with two-dimensional flow conditions. The inlet is located at the upper portion of the left wall and the outlet at the lower portion of the right wall, both with heights corresponding to 25% of the cavity height (0.25 m).

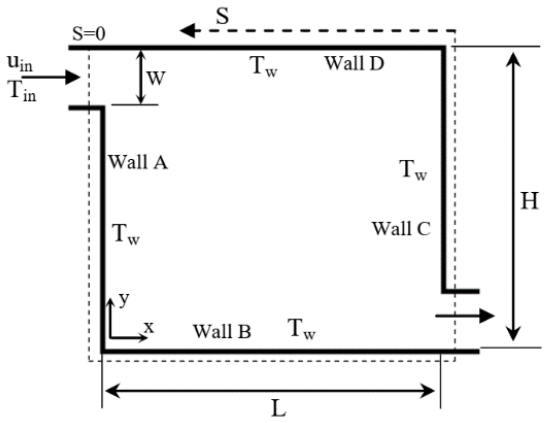


Figure 1. Computational domain. Source: Mioralli et al. (2017).

Boundary conditions were set as follows: inlet temperature $T_{in}=299\ K$, inlet velocity $u_{in}=1.0\ m/s$, and zero pressure gradient at the inlet $(\vec{\nabla}p_{in}=0)$. Wall temperatures were fixed at $T_w=300\ K$ with a no-slip condition for velocity and zero pressure gradient ($\vec{\nabla}p_w=0$). At the outlet, zero temperature and velocity gradients were imposed, with the pressure set to atmospheric ($P_{out}=101{,}325\ Pa$). Initial conditions were $T0=300\ K$, $u_0=0.0\ m/s$, and $P_0=101{,}325\ Pa$.

In OpenFOAM, *Re* and *Pr* can be specified in the *thermophysicalProperties* file. The Prandtl number is entered directly in the solver configuration, while the Reynolds number is indirectly defined through the kinematic viscosity, inlet velocity, and cavity height. For the numerical solution of the pressure–velocity coupling, the Semi-Implicit Method for Pressure-Linked Equations (SIMPLE) algorithm was used, specifically the *buoyantSimpleFoam* variant, to solve Eqs. (1) to (3). The *upwind* scheme was applied for discretizing convective terms, and a linear scheme for diffusive terms, in all three equations. According to OpenFOAM (2025), this solver can handle incompressible flows using the finite volume method, with second-order spatial accuracy, and employs the Gauss–Seidel method for solving the linear systems for velocity, pressure, and temperature under the steady-state flow assumption.

3 Results

The cavity was virtually divided into four subdomains, as shown in Fig. 2, each measuring 1.0 m × 0.25 m, to facilitate the spatial and geometric identification of the inlet and outlet. Consequently, the two-dimensional mesh was subdivided into four distinct blocks. In the upper block, referred to as Block I, the flow inlet was placed at the upper portion of the left wall. In the lower block, referred to as Block IV, the outlet was positioned at the lower portion of the right wall. Each of the four blocks was discretized into control volumes according to the specific requirements of each simulated mesh.

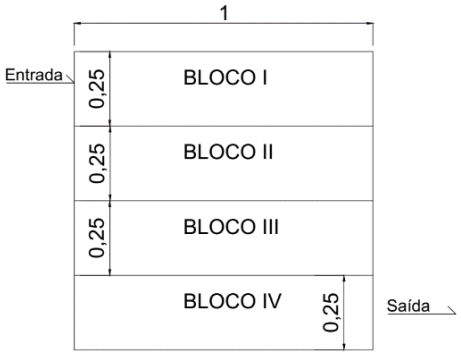
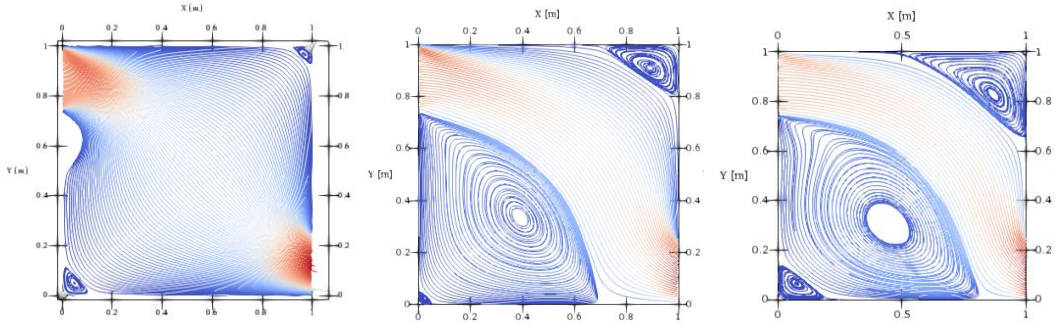


Figure 2. Division of the computational domain into blocks, each subdivided according to the predefined number of control volumes in the mesh.

In the work of Mioralli et al. (2017), the physical parameters of the flow were varied according to the three Reynolds numbers (50, 100 and 500) and three Prandtl numbers (0.7, 3.0 and 5.0), yielding nine possible computational simulations.

As a qualitative analysis, Fig. 3 shows the streamlines (colored by velocity magnitude) obtained for simulations 3, 6, and 9, *i.e.*, Pr = 5.0 and different Reynolds numbers. The results indicate the presence of a primary flow stream passing directly from the inlet to the outlet of the computational domain; consequently, this region experiences the highest rate of thermal convection. Furthermore, increasing the Reynolds number revealed the growth of recirculation zones in the lower left corner, the appearance of secondary recirculations in the same corner, and an increase in the size of these recirculation regions for Re = 100 and Re = 500. An increase in the recirculation in the upper right corner was also observed. All these phenomena are consistent with the findings of Mioralli et al. (2017).

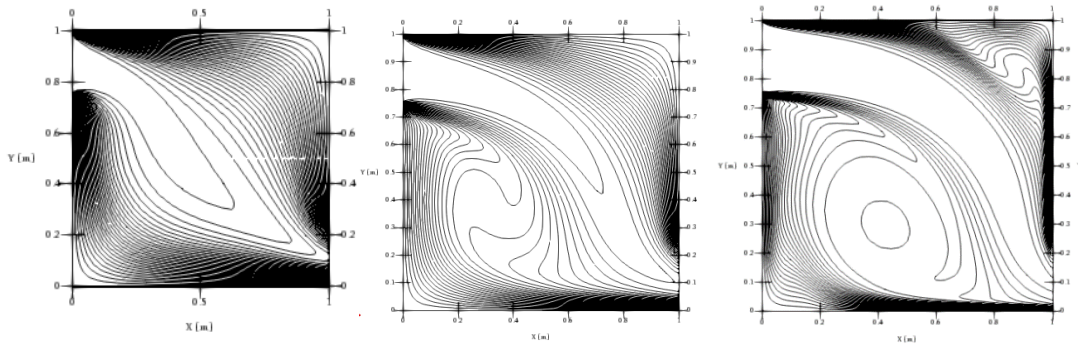


a) Re = 50 b) Re = 100 c) Re = 500

Figure 3. Streamlines with Pr = 5.0.

Temperature contours obtained for the Pr=5.0 were also compared with those from Mioralli et al. (2017), as illustrated in Fig. 4. For Pr = 5.0 (Fig. 4a), the temperature gradients near the inlet and outlet become more intense. When Re is increased from 50 to 100 (Figs. 4a–4b), the same pattern is observed: as Pr increases, the inlet and outlet zones become more distinct, and the contours of the central recirculation become more pronounced. For Re

= 500 (Fig. c), further intensifies temperature gradients, particularly near the walls and inlet/outlet regions. We note that at the interface between the main flow and the central recirculation, a pronounced temperature gradient exists, indicating thermal energy exchange between the incoming flow and the recirculation zone.



a) Re = 50 b) Re = 100 c) Re = 500

Figure 4. Temperature contours with Pr = 5.0.

Figure 5 compares the local Nusselt number distributions along each surface of the computational domain for Re = 50, Re = 100, and Re = 500.

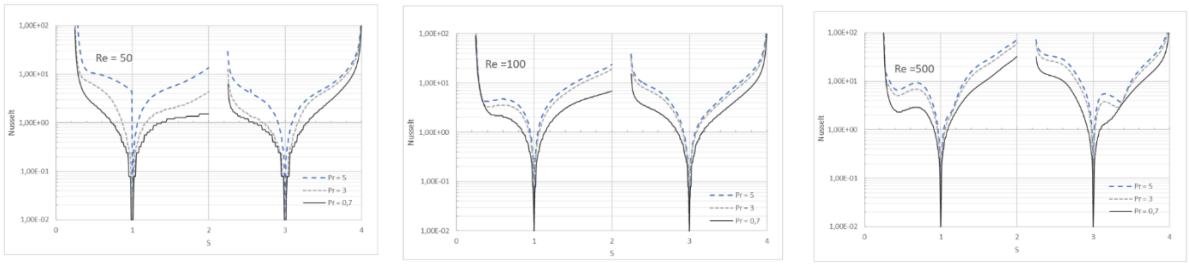


Figure 5. Local Nusselt number for Re = 50, Re = 100, and Re = 500.

The plots in Fig. 5 show that, regardless of Reynolds number, the local Nusselt number reaches its maximum at the inlet and outlet, decreasing along the wall until it becomes zero at the lower left and upper right corners, an effect caused by the formation of secondary recirculation zones. It is also evident that, for a fixed Re, increasing Pr results in a higher local Nusselt number, indicating an increase in heat transfer through the walls.

Finally, once the mean local Nusselt numbers for each wall were obtained for all nine simulations, the overall mean Nusselt number for the cavity was calculated, as shown in Tab. 2.

Table 2. Overall mean Nusselt number for the nine simulations.

	Work	**Pr**		
		0,7	**3.0**	**5.0**
Re = 50	This Work	2,77	4,48	6,23
	Mioralli et al. (2017)	3,16	5,53	6,65
	Difference	-0,1388	-0,2354	-0,0682
Re = 100	This Work	4,27	7,63	8,99
	Mioralli et al. (2017)	4,23	7,42	9,19
	Difference	0,0094	0,0270	-0,0221
Re = 500	This Work	9,04	16,53	20,22
	Mioralli et al. (2017)	8,69	16,00	20,07
	Difference	0,0390	0,0319	0,0074

The largest difference between the present work and Mioralli et al. (2017) was observed for Re = 50 and Pr = 3.0, likely due to differences in the temperature distribution behavior along the floor and right wall.

4 Conclusion

This study investigated the application of the OpenFOAM software for the numerical simulation of forced convection flows in a ventilated square cavity, with the objective of validating the adopted computational model against the benchmark results of Mioralli et al. (2017). The validation process involved reproducing the forced convection problem under various Reynolds and Prandtl number combinations, analyzing both qualitative and quantitative parameters, such as velocity fields, temperature distributions, and local and mean Nusselt numbers.

The comparison of streamlines, temperature contours, and local Nusselt distributions demonstrated that the main flow features, primary jet, recirculation zones, and heat transfer patterns, were successfully captured. Quantitative comparisons revealed maximum velocity errors below 4.0% and consistent trends for local and mean Nusselt numbers across all tested Re and Pr combinations.

Future work should extend the present approach to three-dimensional configurations and incorporate additional physical effects, such as buoyancy-driven flows, humidity transport, and turbulence modeling, aiming to further enhance the predictive capabilities of CFD tools in HVAC-R system design and optimization.

Acknowledgements. The authors gratefully acknowledge FAPEG and CEHTES for the scholarship support provided. We also acknowledge FUNAPE, PPGMEC, and CAPES for financial support. Furthermore, we thank LATEF and LaMCAD for granting access to their physical infrastructure, which was essential for the execution of this research.

Authorship statement. The authors hereby confirm that they are the sole liable persons responsible for the authorship of this work, and that all material that has been herein included as part of the present paper is either the property (and authorship) of the authors, or has the permission of the owners to be included here.

References

[1] A. Castro Silva, “Numerical analysis of cold storage chambers using FLUENT®”. *Journal of Thermal Engineering*, vol. 45, n. 2, pp. 123–134, 2018.
[2] S. C. Chapra and R. P. Canale. *Numerical Methods for Engineers*. McGraw-Hill, 2008.
[3] C. I. P. Martínez and A. C. Poveda, “Challenges and opportunities in the management of refrigeration and air conditioning systems to reduce environmental impacts in the Colombian health sector”. *International Journal of Refrigeration*, vol. 141, pp. 54–65, 2022.
[4] S. Limane, S. Benhadid, and A. Raji, “Thermal ventilation in a rectangular cavity heated from below: validation using OpenFOAM”. *International Journal of Heat and Mass Transfer*, vol. 78, pp. 245–256, 2014.
[5] S. Limane, S. Benhadid, and A. Raji, “CFD simulation of moist airflows and heat–mass transfer in an indoor swimming pool using OpenFOAM”. *Energy and Buildings*, vol. 150, pp. 1–12, 2017.
[6] R. M. Mioralli, L. R. Santos, and R. L. Pimentel, “Numerical study of forced convection in ventilated cavities: benchmark validation,” *International Journal of Numerical Methods for Heat and Fluid Flow*, vol. 27, n. 6, pp. 1235–1252, 2017.
[7] P. V. Nielsen. *Flow in air-conditioned rooms: ventilation by displacement*, PhD thesis, Technical University of Denmark, 1976.
[8] F. Petruzziello, A. Grilletto, C. Cilenti, M. Martínez-Angeles, P. Giménez-Prades, A. D. Sorbo, A. Mota-Babiloni, R. Llopis, A. Maiorino, and C. Aprea, “Refrigeration technologies to increase cold chain Sustainability”. *Nature Reviews Clean Technology,* vol. 1, pp. 604–620, 2025.
[9] C. Greenshields, and H. Weller, *Notes on Computational Fluid Dynamics: General Principles,* CFD Direct Ltd, Reading, UK, 2022